Assessment of a simple correction for the long-range charge-transfer problem in time-dependent density-functional theory

Johannes Neugebauer,[a] Oleg Gritsenko,[b] and Evert Jan Baerends[c]
Theoretical Chemistry, Vrije Universiteit Amsterdam, De Boelelaan 1083, 1081 HV Amsterdam, The Netherlands

(Received 13 February 2006; accepted 27 March 2006; published online 1 June 2006)

The failure of the time-dependent density-functional theory to describe long-range charge-transfer (CT) excitations correctly is a serious problem for calculations of electronic transitions in large systems, especially if they are composed of several weakly interacting units. The problem is particularly severe for molecules in solution, either modeled by periodic boundary calculations with large box sizes or by cluster calculations employing extended solvent shells. In the present study we describe the implementation and assessment of a simple physically motivated correction to the exchange-correlation kernel suggested in a previous study [O. Gritsenko and E. J. Baerends J. Chem. Phys. **121**, 655 (2004)]. It introduces the required divergence in the kernel when the transition density goes to zero due to a large spatial distance between the "electron" (in the virtual orbital) and the "hole" (in the occupied orbital). A major benefit arises for solvated molecules, for which many CT excitations occur from solvent to solute or vice versa. In these cases, the correction of the exchange-correlation kernel can be used to automatically "clean up" the spectrum and significantly reduce the computational effort to determine low-lying transitions of the solute. This correction uses a phenomenological parameter, which is needed to identify a CT excitation in terms of the orbital density overlap of the occupied and virtual orbitals involved. Another quantity needed in this approach is the magnitude of the correction in the asymptotic limit. Although this can, in principle, be calculated rigorously for a given CT transition, we assess a simple approximation to it that can automatically be applied to a number of low-energy CT excitations without additional computational effort. We show that the method is robust and correctly shifts long-range CT excitations, while other excitations remain unaffected. We discuss problems arising from a strong delocalization of orbitals, which leads to a breakdown of the correction criterion. © *2006 American Institute of Physics*. [DOI: 10.1063/1.2197829]

I. INTRODUCTION

Time-dependent density-functional theory (TDDFT) has gained a great popularity for the calculation of excitation energies and optical spectra during the past years. It offers a good compromise between computational efficiency and accuracy for many types of applications (see, e.g., Refs. 1–3 and references therein). The growing number of applications to large systems has not only shown the strength but also the weaknesses of TDDFT. One of the major concerns is the complete failure to deal with long-range charge-transfer excitations.

In TDDFT, the excitation energies ω_k are obtained from the eigenvalue problem[4]

$$\mathbf{\Omega F}_k = [\boldsymbol{\mathcal{E}}^2 + 2\boldsymbol{\mathcal{E}}^{1/2}\mathbf{K}\boldsymbol{\mathcal{E}}^{1/2}]\mathbf{F}_k = \omega_k^2 \mathbf{F}_k, \tag{1}$$

where $\boldsymbol{\mathcal{E}}$ is the diagonal matrix of the orbital energy differences of virtual (labels a and b) and occupied (labels i and j) orbitals,

$$\mathcal{E}_{ia,jb} = (\epsilon_a - \epsilon_i)\delta_{ij}\delta_{ab}, \tag{2}$$

$\mathbf{K}$ is the coupling matrix, which—for real orbitals and singlet-singlet excitations in closed-shell molecules—has the elements

$$K_{ia,jb} = \int d\mathbf{r}_1 \int d\mathbf{r}_2 \phi_i(\mathbf{r}_1)\phi_a(\mathbf{r}_1)2 \times \left[\frac{1}{|\mathbf{r}_1 - \mathbf{r}_2|} + f_{\mathrm{xc}}(\mathbf{r}_1, \mathbf{r}_2, \omega)\right]\phi_j(\mathbf{r}_2)\phi_b(\mathbf{r}_2). \tag{3}$$

The exchange-correlation kernel f_{xc} is the functional derivative of the time-dependent exchange-correlation potential with respect to the time-dependent ground-state density, but it is routinely approximated with the simple, time-independent, adiabatic local density approximation (ALDA). However, it leads to a systematic underestimation of excitation energies of long-range charge-transfer (CT) excitations, ω_{CT}. This problem has been discussed in detail before.[5–10]

One way to correct charge-transfer excited states is to include Hartree-Fock (HF) exchange in the exchange-correlation (XC) kernel, i.e., by applying hybrid functionals in the TDDFT calculation,[7,11,12] but if the fraction of the HF exchange is smaller than 100%, only a partial correction is achieved. Consequently, a hybrid approach was suggested, in

[a]Electronic mail: johannes.neugebauer@phys.chem.ethz.ch . Present address: Laboratory of Physical Chemistry, ETH Zurich, Wolfgang-Pauli-Strasse 10, 8093 Zurich, Switzerland
[b]Electronic mail: gritsenk@chem.vu.nl
[c]Electronic mail: baerends@chem.vu.nl

which the potential energy curve for a CT excited state is calculated from a configuration interaction singles (CIS) calculation and is subsequently vertically shifted to match an excitation energy obtained from two self-consistent-field (SCF) density-functional theory (DFT) calculations, converged to different states (ΔSCF-DFT), at a large donor-acceptor distance.[7] This approach has successfully been applied to xanthophyll-chlorophyll dimers[13,14] and complexes of zincbacteriochlorin and bacteriochlorin as well as bacteriochlorophyll and spheroidene.[15] There are, however, two drawbacks of this method: First, three different types of independent calculations are needed to get the whole set of excitation energies, namely, a ΔSCF-DFT calculation for the offset, a CIS calculation for the CT states, and a TDDFT calculation for the remaining states. In particular, the user has to select which states should be taken from the CIS calculation and which from the TDDFT calculation. Second, if applied rigorously, it would require to do one ΔSCF-DFT calculation for each CT state that shall be corrected. This could be a problem, since the optimization to higher-energy CT states will not be a trivial task and might be impossible in many cases. Moreover, the inclusion of exact exchange makes the calculations significantly more demanding for larger systems, as no advantage can be taken of efficient density fitting techniques for the induced potential.[16] This approach might therefore be well suited for cases where a particular charge-transfer state is of interest in the calculation. If the interest is on the contrary in a non-CT state which is hidden among a multitude of CT states, as may occur, e.g., for solvated chromophores,[17] it will not be of much use, since the main problem in those cases is to automatically detect the CT states. Tawada *et al.* suggested a long-range correction to the coupling matrix which is based on the HF exchange.[8,18] Although this leads to an automatic correction of CT excitations, it still has the disadvantage of requiring computationally expensive exchange integrals.

Here, we present a physically motivated correction to the exchange-correlation kernel, which has the property to selectively correct the CT excitation energies and does not require the calculation of any HF exchange integrals. The corrected excitation energy depends on the quantity Δ^A (sometimes called the derivative discontinuity), which can, in principle, be calculated rigorously. Although this is certainly necessary to arrive at a high accuracy for the charge-transfer excitation energies, it is possible to find simple, transition-specific estimates for Δ^A, which can automatically be applied. The main benefit from this simple correction scheme is that low-lying valence excitations are easily isolated from artificially low CT states in one single calculation at a low computational cost. Although this can also be achieved by embedding methods,[17,19] the present exchange-correlation kernel has the advantage that couplings to orbital transitions in the embedding region are fully incorporated.

The present study is organized as follows: In Sec. II the correction to the exchange-correlation kernel and details relevant for its implementation are explained. Section III deals with the proper choice of the quantities needed in the correction scheme for the simple test case of two closed-shell atoms at varying distances. A more complicated benchmark example, a complex consisting of ethylene and tetrafluoroethylene, for which several low-lying CT states need to be corrected, is studied in Sec. IV. The usefulness of our simple correction scheme is then demonstrated for a solvated acetone molecule in Sec. V, before we summarize and conclude in Sec. VI.

II. METHODOLOGY

In Ref. 9, a correction for the exchange-correlation kernel which has the correct asymptotic limit for CT excitations was proposed. An empirical switching function should guarantee that only long-range CT excitations are corrected, which are characterized by the fact that the differential overlap $\phi_i(\mathbf{r})\phi_a(\mathbf{r})$ is close to zero. Furthermore, a simpler approximation for the corrected coupling matrix elements was suggested, which also leads to the correct asymptotic limit

$$K_{ia,jb} = K_{ia,jb}^{\mathrm{ALDA}} + \delta_{ij}\delta_{ab}\exp[-(S_{ia}/S_c)^2] \times\left[-K_{ia,ia}^{\mathrm{ALDA}} + \Delta^A - \frac{1}{R_{ia}} + \frac{(\Delta^A - 1/R_{ia})^2}{2(\epsilon_a - \epsilon_i)}\right], \quad (4)$$

where $K_{ia,jb}^{\mathrm{ALDA}}$ are the uncorrected coupling matrix elements within the adiabatic local density approximation, S_{ia} is the orbital density overlap

$$S_{ia} = \int \phi_i^2(\mathbf{r})\phi_a^2(\mathbf{r})d\mathbf{r}, \quad (5)$$

which measures the magnitude of the differential overlap, S_c is a small empirical parameter to ensure that the correction term (in square brackets) is only switched on if the overlap integral S_{ia} is small, and R_{ia} is the "average distance" between the orbital densities,

$$R_{ia} = \sqrt{X_{ia}^2 + Y_{ia}^2 + Z_{ia}^2}, \quad (6)$$

with

$$X_{ia} = \int [\phi_i^2(\mathbf{r}) - \phi_a^2(\mathbf{r})]x d\mathbf{r} \quad (7)$$

and the corresponding expressions for Y_{ia} and Z_{ia}. The quantity Δ^A, which is the correction applied to the excitation energies in the asymptotic limit of an infinite distance between the electron donor and acceptor in the system, is defined as the difference between the true CT excitation energy ω_{CT} and the TDDFT result in the asymptotic limit when employing the ALDA [it also holds for generalized gradient approximation (GGA) exchange-correlation kernels], $\omega_{\mathrm{CT}}^{\mathrm{ALDA}}$. For the lowest-energy CT transition at an infinite distance, it is given by

$$\Delta^A = \omega_{\mathrm{CT}} - \omega_{\mathrm{CT}}^{\mathrm{ALDA}} \approx I^D - A^A - (\epsilon_A - \epsilon_D) = -A^A - \epsilon_A, \quad (8)$$

where ϵ_A and ϵ_D are the acceptor's lowest unoccupied molecular orbital (LUMO) and the donor's highest occupied molecular orbital (HOMO) energies, respectively, and I^D and A^A are the ionization energy of the donor and the electron affinity of the acceptor, respectively.[9] The latter equality holds, since $I^D = -\epsilon_D$, i.e., the orbital energies of the highest occupied orbitals in the Kohn-Sham theory are strictly equal to vertical ionization potentials.[20,21] For the same reason, we

can write the electron affinity of the acceptor as the negative orbital energy of the HOMO of the negatively charged acceptor ϵ_{A^-} (in case of an initially neutral acceptor), so that $\Delta^A = -A^A - \epsilon_A = \epsilon_{A^-} - \epsilon_A$.

In Ref. 9 it was proposed to use $\Delta^A \approx -\epsilon_A$ as a first approximation. Since the main goal of this study is to apply the asymptotic correction scheme to systems with many charge-transfer excitations hampering a study of intramolecular excitations, we will use the rather simplistic guess $\Delta_a = -\epsilon_a$ for transitions to arbitrary affinity levels ϵ_a on the acceptor fragment. It is obvious that this simple guess can introduce problems especially for higher-lying virtual orbitals, and it will be demonstrated in Section III that more advanced guesses can be found. In order to avoid unphysical corrections for higher-lying virtual orbitals, the asymptotic correction to a certain excitation will only be applied if $\Delta_a - 1/R_{ia}$ is a positive quantity. That is, high-lying charge-transfer excitations, which are usually out of the energy range of interest in our examples, will not be corrected. Another consequence of this choice for Δ_a is that the corrected excitation energy in the asymptotic limit is given by

$$\omega_{\mathrm{CT},ia}^{\mathrm{ALDA+cor}} = \omega_{\mathrm{CT},ia}^{\mathrm{ALDA}} + \Delta_a = -\epsilon_i, \tag{9}$$

so that all CT excitations from a particular donor orbital will have the same excitation energy at long distances.

A more detailed analysis of better choices for Δ_a will be carried out in a subsequent work,[22] whereas in this study we are focusing on the general applicability of the correction scheme in cases where no quantitative but only a qualitative correction of CT states is needed. We will demonstrate that one major problem can be solved even by this simple correction, namely, the fact that low-energy valence transitions are often hidden among a multitude of spuriously low long-range CT excitations in TDDFT calculations for systems consisting of weakly interacting subunits.

As can be seen from Eq. (4), our correction scheme interpolates between the ALDA version and the asymptotically correct version of the exchange-correlation kernel or, to be more precise, the corresponding coupling matrix elements. This means that we need to know the individual diagonal elements of the coupling matrix, $K_{ia,ia}^{\mathrm{ALDA}}$, that shall be corrected. However, these coupling matrix elements are, in many cases, not directly calculated for efficiency reasons. The TDDFT eigenvalue problem [Eq. (1)] is usually solved by subspace iteration methods, most commonly by Davidson-type iterative solutions for the lowest eigenvalues.[23,24] In these methods, matrix-vector products of the coupling matrix $\mathbf{K}$ with a certain test vector $\mathbf{p}_{\mathrm{in}}^k$ describing the excitation to be optimized are calculated,[16]

$$[p_{\mathrm{out}}^k]_{jb} = \sum_{lc} K_{jb,lc}[p_{\mathrm{in}}^k]_{lc}. \tag{10}$$

The output vectors can be expressed as

$$[p_{\mathrm{out}}^k]_{jb} = \int d\mathbf{r}_1 \phi_j(\mathbf{r}_1)\phi_b(\mathbf{r}_1)v_{\mathrm{ind}}^k(\mathbf{r}_1), \tag{11}$$

where

$$v_{\mathrm{ind}}^k(\mathbf{r}_1) = \int d\mathbf{r}_2 \left\{ \left[\frac{1}{|\mathbf{r}_1 - \mathbf{r}_2|} + f_{\mathrm{xc}}^{\mathrm{ALDA}}(\mathbf{r}_1)\delta(\mathbf{r}_1 - \mathbf{r}_2) \right] \times \sum_{lc} [p_{\mathrm{in}}^k]_{lc}\phi_l(\mathbf{r}_2)\phi_c(\mathbf{r}_2) \right\} \tag{12}$$

is the potential induced by the density change described by the test vector $\mathbf{p}_{\mathrm{in}}^k$. The induced potential is, for efficiency reasons, calculated in terms of the fitted density

$$\tilde{\rho}_{\mathrm{in}}^k(\mathbf{r}_2) = \sum_i a_i f_i(\mathbf{r}_2) \approx \sum_{lc} [p_{\mathrm{in}}^k]_{lc}\phi_l(\mathbf{r}_2)\phi_c(\mathbf{r}_2), \tag{13}$$

where a_i and f_i are fit coefficients and functions, respectively (for details, see Ref. 16). Therefore, the summation in Eq. (10) is carried out implicitly without calculating individual matrix elements $K_{ia,jb}$. However, by combining Eqs. (4) and (10) we see that the expression for the corrected matrix-vector products still contains particular matrix elements $K_{ia,ia}^{\mathrm{ALDA}}$,

$$[p_{\mathrm{out}}^{k,\mathrm{cor}}]_{ia} = [p_{\mathrm{out}}^{k,\mathrm{ALDA}}]_{ia} + [p_{\mathrm{in}}^k]_{ia} \exp[-(S_{ia}/S_c)^2] \times \left[-K_{ia,ia}^{\mathrm{ALDA}} + \Delta^A - \frac{1}{R_{ia}} + \frac{(\Delta^A - 1/R_{ia})^2}{2(\epsilon_a - \epsilon_i)} \right]. \tag{14}$$

Our correction, thus, puts the additional problem that not only the matrix-vector products but also the diagonal elements of the matrix $\mathbf{K}$ need to be calculated. A number of facts can be exploited to reduce the computational effort for this task. The matrix elements are directly evaluated in a molecular orbital basis. In contrast to this, the fitting of the induced density $\tilde{\rho}_{\mathrm{in}}^k$ [Eq. (13)] and the calculation of the matrix elements of Eq. (11) is usually carried out in an atomic orbital basis to make use of linear scaling techniques.[16,25] A second point is that we only want to correct the coupling matrix elements when $K_{ia,ia}^{\mathrm{ALDA}}$ is small due to the vanishing differential overlap. In that case, also the orbital density overlap will be small. Therefore, we approximate $K_{ia,ia}^{\mathrm{ALDA}} \approx 0$ if $S_{ia} < S_c/100$. Note that S_c *should* be chosen in such a way that $K_{ia,ia}^{\mathrm{ALDA}}$ is negligible if the correction is fully switched on. This is a basic assumption in the phenomenological correction scheme applied here. Moreover, the correction will only be applied if the expression

$$T_{ia} = \exp[-(S_{ia}/S_c)^2] \left[\Delta^A - \frac{1}{R_{ia}} + \frac{(\Delta^A - 1/R_{ia})^2}{2(\epsilon_a - \epsilon_i)} \right] \tag{15}$$

is larger than a certain threshold (default: 1.0×10^{-6} a.u.); otherwise, the correction will not be important anyway. By testing the magnitudes of S_{ia} and T_{ia}, we can therefore reduce the number of explicitly needed diagonal $\mathbf{K}$-matrix elements significantly. As a further criterion, we might exploit the fact that mixings with high-energy transitions, which are not optimized in the Davidson procedure, are typically negligibly small, so that their diagonal $\mathbf{K}$-matrix elements need not be corrected.

A problem can occur in calculations for very large systems: Among the n initial guess vectors for the subspace iteration, there might only be a very small number of non-CT

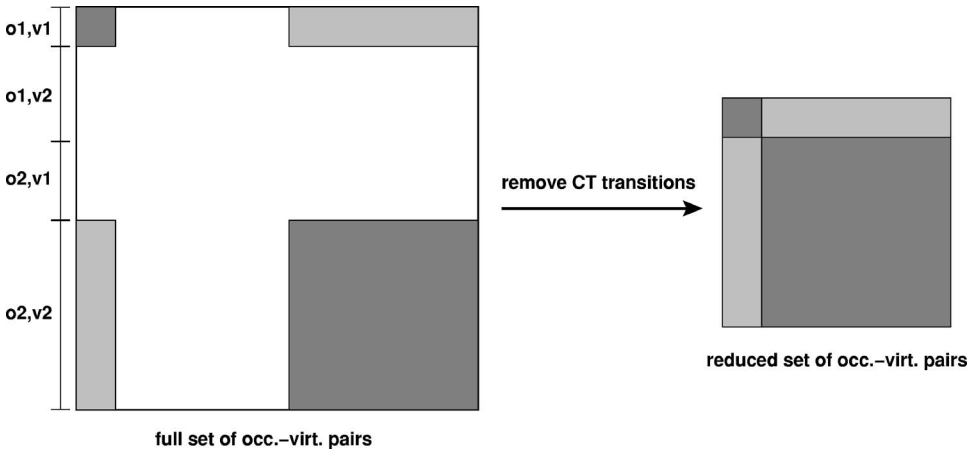

FIG. 1. Schematic representation of the (uncorrected) coupling matrix for a system consisting of two fragments with a large separation. Left: full coupling matrix in the basis of all occupied (o1/o2)-virtual (v1/v2) orbital pairs for fragments 1 and 2. Right: coupling matrix after the removal of the orbital pairs corresponding to CT excitations. The white areas correspond to matrix elements that will be (close to) zero due to a zero differential overlap.

transitions. Subsequent iterations will, in those cases, almost always produce excitations which are lower in energy than the initial ones, since many of them are shifted by the kernel correction. The reason for this is that the calculation starts with a very bad guess for those excitations, since the initial vectors are good guesses for the lowest *n uncorrected* excitations. Since there might be many excitations below the corrected CT excitations which are described by the initial guess vectors, subsequently lower and lower roots of the $\mathbf{\Omega}$ matrix may be found. This will result in a rather poor convergence for the lowest excitation energies. A solution is to determine the orbital transitions for which guess vectors are created not on the basis of the orbital energy differences but to use a corrected guess energy

$$\Delta E_{ia}^{\text{guess}} = \sqrt{(\epsilon_a - \epsilon_i)^2 + \exp[-(S_{ia}/S_c)^2]\left[2(\epsilon_a - \epsilon_i)\left(\Delta^A - \frac{1}{R_{ia}}\right) + \left(\Delta^A - \frac{1}{R_{ia}}\right)^2\right]}, \tag{16}$$

which is the correct excitation energy under the assumptions that (i) no off-diagonal couplings exist for the orbital transition $\phi_i \rightarrow \phi_a$ and that (ii) the diagonal elements of the uncorrected coupling matrix, $K_{ia,ia}^{\text{ALDA}}$, are sufficiently small when the correction term is significant. Equation (16) should provide a reasonable estimate for the excitation energies of both CT and non-CT transitions. For the latter, Eq. (16) will be reduced to the normal excitation guess energy $\Delta E_{ia}^{\text{guess}} = \epsilon_a - \epsilon_i$. This guess energy should be used not only to determine which orbital transitions will be the lowest in energy but also to set up the preconditioner in the Davidson procedure.[23,24] In the long-range limit, where $S_{ia} \approx 0$, Eq. (16) results in the following guess for CT excitation energies;

$$\Delta E_{ia}^{\text{CT}} = \sqrt{(\epsilon_a - \epsilon_i)^2 + 2(\epsilon_a - \epsilon_i)\left(\Delta^A - \frac{1}{R_{ia}}\right) + \left(\Delta^A - \frac{1}{R_{ia}}\right)^2} \tag{17}$$

$$= \epsilon_a - \epsilon_i + \Delta^A - \frac{1}{R_{ia}}. \tag{18}$$

If the differential overlap between the orbitals involved is vanishingly small, this guess energy will be identical to the optimized excitation energy, since the couplings to other orbital transitions will be small. This suggests that—based on the quantities S_{ia}—one might arrive at an even simpler scheme (not used here), in which the space of orbital transitions is restricted to those for which S_{ia} is above a certain threshold. If it is smaller, the guess energies will be sufficiently close to the optimized excitation energies, and the corresponding orbital transitions can be considered to build isolated 1×1 blocks of the $\mathbf{\Omega}$ matrix.

To illustrate this further, assume that the distance between the fragments is sufficiently large. The (uncorrected) coupling matrix will then have the structure depicted in Fig. 1. All elements for occupied-virtual orbital pairs located on different fragments will be zero. With that knowledge (based on S_{ia}), we might remove all orbital pairs corresponding to CT transitions to get to the reduced set of occupied-virtual orbital pairs. The correction for the CT excitations can be applied directly to the orbital energy differences. This will reduce the CPU and memory requirements for calculating the matrix-vector products in the subspace iteration procedure. For intermediate distances, some of the CT-like orbital pairs might still be included in the basis for the Davidson diagonalization.

All calculations in this work are carried out using a modified version of the program package ADF,[26,27] in which the asymptotic correction to the coupling matrix [Eq. (4)] was implemented. For TDDFT calculations, we use the "statistical averaging of (model) orbital potentials" (SAOP) potential[28–30] in combination with the TZP or TZ2P basis sets

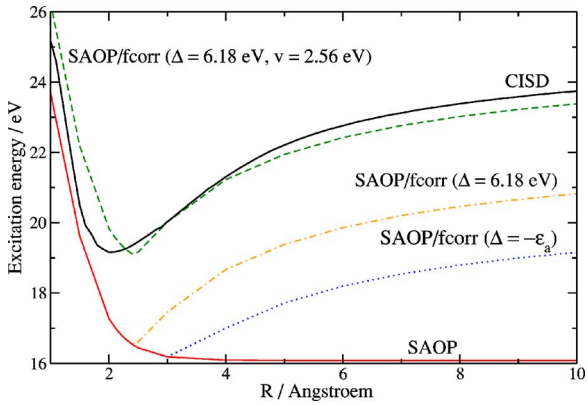

FIG. 2. Excitation energies for the system He···Be as a function of the internuclear distance R from SAOP/TZ2P calculations [fcorr: f_{xc} corrected according to Eq. (4)]. CISD data from Ref. 9 are given for comparison.

from the ADF basis set library.[26] Ground-state energies are computed with the Becke-Perdew-Wang (BPW91) exchange-correlation functional,[31,32] since no corresponding energy expression is defined for the SAOP potential.

III. A SIMPLE TEST SYSTEM: He···Be

As a simple test system, we use the He···Be system, for which an initial study was already presented in Ref. 9.

In Fig. 2 we show the excitation energies for the $1s(\mathrm{He}) \rightarrow 2p_\pi(\mathrm{Be})$ transition of the He···Be system as a function of the internuclear distance. These were obtained with SAOP/TZ2P calculations and different estimates for the quantity Δ^A. Based on some initial tests, the switching parameter S_c was set to 0.0001 a.u. in these calculations. Additionally, the configuration interaction singles and doubles (CISD) reference values from Ref. 9 are plotted. As mentioned before, we use $\Delta_a \approx -\epsilon_a$ as a first approximation for the kernel correction. For the excitation under study here, this means that in the asymptotic limit the excitations will be shifted by $-\epsilon_{2p_\pi}(\mathrm{Be})=4.52$ eV, as calculated with SAOP/TZ2P.

Already with this simple correction, we observe a qualitatively correct Coulombic behavior in the asymptotic limit, although the difference with respect to the CISD curve is still in the order of 4.5 eV at distances larger than 4 Å. The asymptotically corrected excitation energies presented in Ref. 9 showed a much better agreement with the CISD values for two reasons: First, a more sophisticated guess was used for the asymptotic shift, $\Delta_a=\Delta^{\mathrm{Be}} \approx 0.23$ eV $-\epsilon^{\mathrm{acc}}_{2p_\pi(\mathrm{Be})}=6.18$ eV. Here, $\epsilon^{\mathrm{acc}}_{2p_\pi(\mathrm{Be})}=-5.95$ eV is the orbital energy from an accurate Kohn-Sham (KS) solution for the Be atom. The electron affinity $A^{\mathrm{Be}}=-0.23$ eV is taken from Ref. 33. As can be seen from Fig. 2, this corrects the former results towards the CISD reference, but there are still differences of ≈3 eV for long distances. Second, the curve in Ref. 9 was corrected for the fact that—with the particular Kohn-Sham potential used—already the zero-order approximation (the orbital energy difference $\epsilon_{2p_\pi(\mathrm{Be})}-\epsilon_{1s(\mathrm{He})}$) is too small for the system under study. Instead of the SAOP/TZ2P result for this difference in the long-range limit (16.08 eV), the "ideal" orbital energy difference was estimated from the ionization energy of He and the value of $\epsilon^{\mathrm{acc}}_{2p_\pi(\mathrm{Be})}$, which results to 18.64 eV. The fourth curve in Fig. 2 was therefore obtained by applying a vertical shift of 2.56 eV (which is the difference between these zero-order guesses) to the results obtained with SAOP/TZ2P and $\Delta_a=6.18$ eV in the correction to the exchange-correlation kernel. This curve closely follows the CISD data not only in the asymptotic limit but also close to the minimum excitation energy.

It should be emphasized that the latter correction is necessary only because of the shortcomings of the exchange-correlation potential for the current system and not due to deficiencies of the correction scheme for the exchange-correlation kernel.

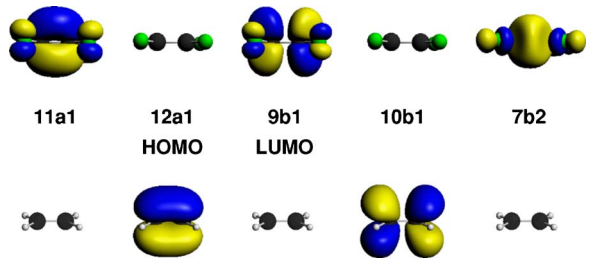

FIG. 3. Isosurface plots of orbitals around the HOMO-LUMO gap involved in some of the low-lying CT excitations of the ethylene-tetrafluoroethylene complex (ascending orbital energies from left to right; distance: 10 Å).

IV. ETHYLENE-TETRAFLUOROETHYLENE

A second benchmark system for the problem of charge-transfer excitations in TDDFT is the complex of ethylene and tetrafluoroethylene. It was shown in Ref. 7 that typical exchange-correlation potentials, even asymptotically correct ones, show a large error for the low-lying charge-transfer states of this system. A partial correction could be observed for hybrid functionals, but the correct asymptotic behavior was only recovered when including the full Hartree-Fock exchange in the exchange-correlation kernel, i.e., in a CIS calculation. Isosurface plots of some of the most important orbitals around the HOMO-LUMO gap are depicted in Fig. 3.

In Figs. 4 and 5 we show the excited-state potential energy curves for irreducible representations (irreps) A_1 and B_1 of the C_{2v} complex along the intermolecular separation coordinate calculated using SAOP/TZP with and without the kernel correction. There are no low-lying (below 8.5 eV) states in irrep A_2, and the excitations in irrep B_2 are given in Fig. S1 of the supplementary material,[34] since no particular additional information about the performance of the correction scheme is contained in that figure. In contrast to the He–Be system, where the pure excitation energies were shown (for comparability to the CISD reference), we show here the usual energy curves by adding to the excitation energies in this case the change in ground-state energies along the distance coordinate. The ground-state energy for a separation of 10 Å was set to zero.

Figure 4 contains the lowest adiabatic potential energy curves for irrep A_1 and will be discussed in some more detail, since there are less states in the interesting energy region than for the other irreps. In the diagram showing the uncor-

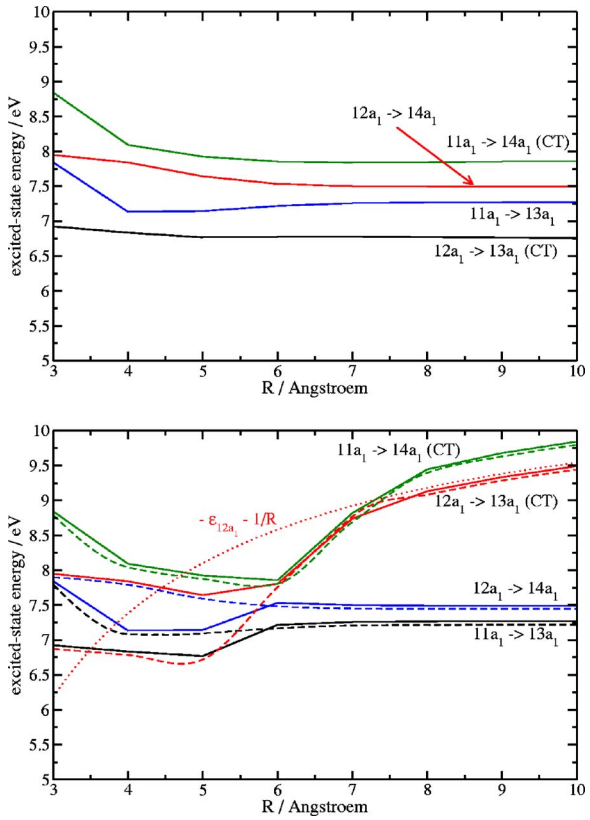

FIG. 4. Adiabatic excited-state potential energy curves (solid lines) for irrep A_1 of the ethylene-tetrafluoroethylene complex (SAOP/TZP; zero point: ground-state energy at 10 Å). Top: no kernel correction; bottom: kernel correction applied. Labels correspond to the character of the excitation at a distance of 10 Å; the character of the excitations may change due to avoided crossings. In the lower diagram, also a pure $-1/R$-like curve for the $12a_1 \rightarrow 13a_1$ state (dotted line; shifted by +0.05 eV for clarity of presentation) as well as "intuitive" diabatic states are shown. The latter curves connect data points of states with similar characters (dashed lines; shifted by −0.05 eV for clarity of presentation).

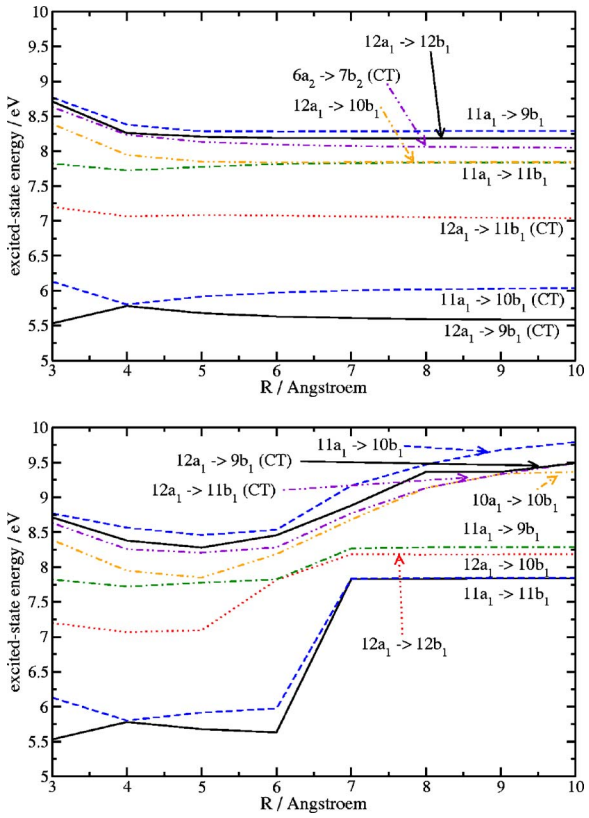

FIG. 5. Adiabatic excited-state potential energy curves for irrep B_1 of the ethylene-tetrafluoroethylene complex (SAOP/TZP; zero point: ground-state energy at 10 Å). Top: no kernel correction; bottom: kernel correction applied. Labels correspond to the characters of the excitation at a distance of 10 Å; the character of the excitations may change due to avoided crossings.

rected curves, all potential energy curves are very flat and show only very small variations with increasing distance. While this is expected for the intramolecular valence transitions $11a_1 \rightarrow 13a_1$ (tetrafluoroethylene) and $12a_1 \rightarrow 14a_1$ (ethylene), the intermolecular charge-transfer excitations $11a_1 \rightarrow 14a_1$ (tetrafluoroethylene $\rightarrow$ ethylene) and $12a_1 \rightarrow 13a_1$ (ethylene $\rightarrow$ tetrafluoroethylene) are also almost independent of the distance. In the second diagram it can be seen that the corrected curves agree with the uncorrected results up to a distance of ≈5 Å. Between 5 and 6 Å, however, the correction is switched on and pushes the charge-transfer excitations to higher energies, so that avoided crossings occur. To guide the eye through these avoided crossings, we also draw "intuitive" diabatic potential energy curves connecting data points of states with similar characters (dashed lines). From these lines it becomes apparent that the valence transitions remain at low energies, while the charge-transfer excitations are selectively increased in energy. Although the position of the avoided crossings depends on the choice of our switching parameter S_c, it is obvious that the long-range behavior of the excited-state energies properly has a Coulomb shape, as is demonstrated by the additional $-1/R$-like curve depicted in that figure.

When comparing to the results obtained with the TDDFT-CIS hybrid approach in Ref. 7, it becomes apparent that the corrected CT state shown in that work basically has a $-1/R$-like behavior over the full R range between 4 and 10 Å. In our case, the CT-like states show many avoided crossings and interactions with other states, so that the Coulombic shape of the excited-state potential energy curve, even in the intuitive diabatic picture, gets lost at short distances. In order to assess whether our correction scheme leads to unphysical results at short distances, we carried out coupled-cluster calculations for the singlet excitations of the $A1$ symmetry using the CC2 model[35,36] and Ahlrichs' basis set of a valence triple-ζ quality with one set of polarization functions (TZVP).[37,38] The (linear response) CC2 calculations for ground and excited states have been carried out using the program package DALTON.[39] The eight lowest-energy orbitals, i.e., the $1s$ orbitals of carbon and fluorine atoms, were kept frozen in the coupled-cluster calculations.

The resulting potential energy curves are shown in Fig. 6. It can be seen that the CC2 excitation energies are, in general, larger than the DFT excitation energies. However, it should be mentioned that initial tests with basis sets of a double-ζ quality indicated that the CC2 excitation energies are rather sensitive to the quality of the basis set used, where larger basis sets lead to a decrease in excitation energies. Since the aim of this calculation is only to provide a basis for a qualtitative comparison, and since the memory require-

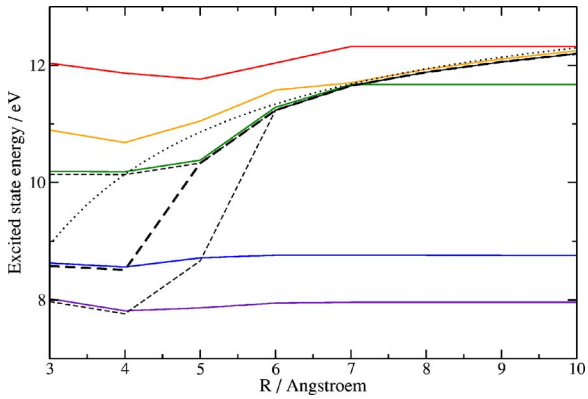

FIG. 6. Adiabatic excited-state potential energy curves (solid lines) for irrep A_1 of the ethylene-tetrafluoroethylene complex (CC2/TZVP; zero point: ground-state energy at 10 Å). We also show a pure $-1/R$-like curve for the CT-state (dotted line; shifted by +0.05 eV for clarity of presentation) as well as the "intuitive" diabatic potential energy curve for the lowest CT-like transition (dashed lines; shifted by −0.05 eV for clarity of presentation). For short distances, the character of this excitation spreads over the three lowest excitations in this irrep (indicated by additional dashed lines).

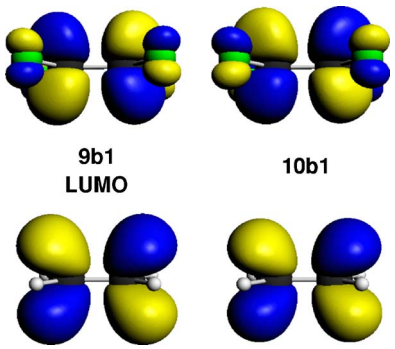

FIG. 7. Isosurface plots of the π^* orbitals of the ethylene-tetrafluoroethylene complex showing a pronounced mixing for a distance of 5 Å.

ments for larger calculations are quite demanding, we refrain from using even larger basis sets for these coupled-cluster calculations. Figure 6 also contains an intuitve diabatic curve connecting data points with the same character as the lowest CT state (identified by its Coulombic shape in the long-range limit) as well as a $-1/R$-like curve. It can be seen that also these *ab initio* calculations predict strong deviations from the Coulombic behavior at short and medium distances (up to ≈5 Å). At short distances, the character of the CT state spreads over the lowest three excitations, demonstrating that interactions between different excited states play a role. Similar to the results obtained with our correction scheme, the CT state is of a lower energy than the $-1/R$-like curve for intermediate distances (4 to 6 Å). The TDDFT results with the default switching function show this deviation from the Coulombic curve at somewhat larger distances (6–7 Å), which suggests that the correction sets in at too low orbital density overlaps. Indeed, a better switching function might be obtained by fitting to such *ab initio* reference calculations. For this work, we restrict ourselves to the default parametrization, which ensures that the asymptotic correction to the exchange-correlation kernel is applied in a "safe" manner; i.e., it is only switched on if the transition under consideration is, without any doubt, of a charge-transfer type.

Similar observations as found for the A_1 states can be made for the other two irreducible representations shown: In irrep B_1, only three out of the lowest seven excitations are of an intramolecular valence type for large separations ($11a_1 \rightarrow 11b_1$, $12a_1 \rightarrow 10b_1$, and $11a_1 \rightarrow 9b_1$), while all other excitations are pushed to energies >9 eV, including the three lowest excitations in the uncorrected case (note that no "diabatic" representations are given in this case for clarity of presentation). Note that the $10a_1 \rightarrow 10b_1$ excitation is not a CT excitation. It is only included in the diagram since it is among the lowest eight excitations at long distances (but not at short distances due to avoided crossings). Also in irrep B_2, there are only three out of the lowest seven excitations which remain uncorrected due to their valence character in the long-range limit ($11a_1 \rightarrow 7b_2$, $6a_2 \rightarrow 10b_1$, and $12a_1 \rightarrow 8b_2$). Higher-lying CT states are not corrected (see Fig. S1 in the supplementary material[34]): The $12a_1 \rightarrow 9b_2$ excitation energy was not affected by the kernel correction. This is due to the fact that the correction $\Delta_a - 1/R_{ia}$ would be negative for this transition, with the particular choice for Δ_a made here. As has been explained in Sec. II, the kernel correction is automatically suppressed in such cases.

The correction is typically switched on in an intermediate region of 4–6 Å, depending on the exact nature of the transition. For larger distances, the asymptotic correction fully replaces the ALDA kernel for long-range CT excitations, so that characteristic Coulombic potential energy curves are obtained, while the energies of the intramolecular valence excitations are not affected and are independent of the intermolecular separation. In both irreducible representations, a multitude of avoided crossings occurs due to the fact that the CT-like excitations have low excitation energies at short distances, where the correction function is not applied due to the larger orbital density overlap. Although it is clearly necessary to find more suitable guesses for Δ_a to determine the excitation energies for the long-range CT states quantitatively, already the simple guess applied here is useful to separate the lowest valence excitations from the artificially low charge-transfer excitations. The latter are selectively and automatically shifted to higher energies, and the shapes of the potential energy curves have the correct behavior. This is an important prerequisite for a practically applicable charge-transfer correction.

A problem can be recognized in Fig. 5: The lowest two curves in irrep B_1 correspond to the $11a_1 \rightarrow 10b_1$ and $12a_1 \rightarrow 9b_1$ transitions in the long-range limit. When the correction is applied, these transitions remain uncorrected up to a distance of 6 Å. The reason for this rather strange-looking behavior is that there is a substantial delocalization of the virtual orbitals between the different subsystems for intermediate distances. The π^* orbitals of ethylene and tetrafluoroethylene mix at intermediate distances (around 5 Å), so that the molecular orbitals extend over both fragments. This can be seen from the isosurface plots of the $9b_1$ and $10b_1$ orbitals (the π^* orbitals) in Fig. 7. The average distance R_{ia} between the highest occupied orbitals, which are still localized on one of the fragments, and the delocalized orbitals is not very large (between 2.2 and 2.8 Å). Also, the orbital density over-

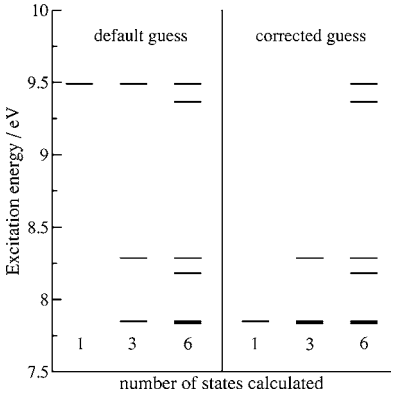

FIG. 8. Excitation energies obtained for different numbers of optimized states in irrep B_1 of the ethylene-tetrafluoroethylene complex. Left: default guess (orbital energy differences) used to construct guesses for the lowest excitations; right: corrected guess [Eq. (16)] applied.

lap S_{ia} is more than 60 times larger for transitions from the HOMO or HOMO-1 to these orbitals than the switching parameter S_c, so that the asymptotic correction is not applied. It should be noted that this is not primarily a parametrization problem, since the orbital overlap is comparable to other orbital pairs localized on one of the fragments only, so that the physical conditions for fully applying the asymptotic correction are clearly not valid in this example. A possible way to correct for such problems could be an intermediate localization step, particularly in cases of purely symmetry-driven delocalization. It has recently been shown that TDDFT methods fail for these systems even if no net charge transfer occurs.[40]

If we are interested in the lowest valence transitions only, there is another point to take care of: The computational cost increases with the number of excitations to be determined, so that we usually want to keep the number of states small. On the other hand, that increases the chance of missing a low-lying state, especially if the guess for this excitation is bad. In particular, in cases of symmetric molecules, there might only be a few excited states optimized per irrep, so that in each irrep there is a danger of missing important low-lying excitations. The construction of the guess vectors is usually based on the zero-order guess for the excitation energies, i.e., the orbital energy differences between occupied and unoccupied orbitals. These zero-order guesses are also used to construct a diagonal guess for the matrix $\mathbf{\Omega}$, which is used for preconditioning in the iterative solution of the eigensystem. Hence, they influence not only the type of excitations which are optimized but also the convergence characteristics. For the excitations in irrep B_1 at an intermolecular distance of 10 Å, this is demonstrated in Fig. 8. Shown are the excitation energies obtained when calculating one, three, or six excited states in that irrep, either with the default zero-order guess or with the corrected guess according to Eq. (16). With the normal orbital energy difference guess, we get the $12a_1 \rightarrow 9b_1$ excitation if only one root is requested, since this is the excitation with the lowest orbital energy difference (5.58 eV). However, the asymptotic correction shifts this excitation to 9.49 eV due to its CT nature. With the corrected guess energy, we obtain a much lower B_1 excitation at 7.85 eV, which is the $12a_1 \rightarrow 10b_1$ transition. Also this is not the lowest excitation, a problem that can occur in subspace iteration methods for the highest among the optimized roots. But the problem is much more severe when using the wrong guess. Only when the lowest six excitations in this irrep are calculated we get the same excitations with both types of guesses.

TABLE I. Number of matrix-vector products needed to converge n roots (irrep B_1) in the TDDFT calculation. A: default zero-order guess used to construct lowest-energy eigenvectors and preconditioner; B: guess vectors based on corrected guess energies [Eq. (16)]; and C: guess vectors and preconditioner based on Eq. (16). Note that scheme A converges to eigenvalues different from those obtained in schemes B and C for small n (see Fig. 8).

n	A	B	C
1	2	6	7
3	24	18	18
6	72	48	30
10	410	50	50
20	140	100	100

Table I shows the number of matrix-vector products that have to be carried out in order to converge the excitation energies. They are a direct measure for the quality of the initial guess vectors and the preconditioner. If only one state is optimized, the default guesses based on orbital energy differences lead to a rapid convergence, since the optimized state is a long-range CT state which shows almost no interaction with any other orbital transition. However, the optimized state is not the desired lowest-energy state. The valence excitation obtained with the corrected guess shows some small couplings, so that more iterations and more matrix-vector multiplications are needed for convergence. For larger numbers of roots to be optimized the corrected guess always leads to a faster convergence than the default guess, although the influence of the correction to the preconditioner is apparently small. The worst case seems to be the calculation with ten roots, in which 410 matrix-vector products are needed. This calculation converges correctly to the ten lowest excitations in irrep B_1, but obviously the guess vectors correspond to other orbital transitions, so that a large number of additional basis vectors is needed to correct this. For 20 excitations, the situation is better again, most probably because similar guess vectors are chosen independently of the type of guess energy used (although the order in which these excitations are according to their guess energy will be different). But still, about 40 matrix-vector multiplications are saved by using the corrected guess energy criterion.

V. SOLVATED ACETONE

The main purpose of this work is to investigate the utility of the kernel correction scheme for solvated molecules. In such systems, many spuriously low charge-transfer excitations can occur, so that even a qualitative correction can be of great value if it can selectively correct CT states. As an example, we study acetone surrounded by several water molecules. The test system, which consists of one acetone and 20 water molecules, is depicted in Fig. 9. It is a finite substruc-

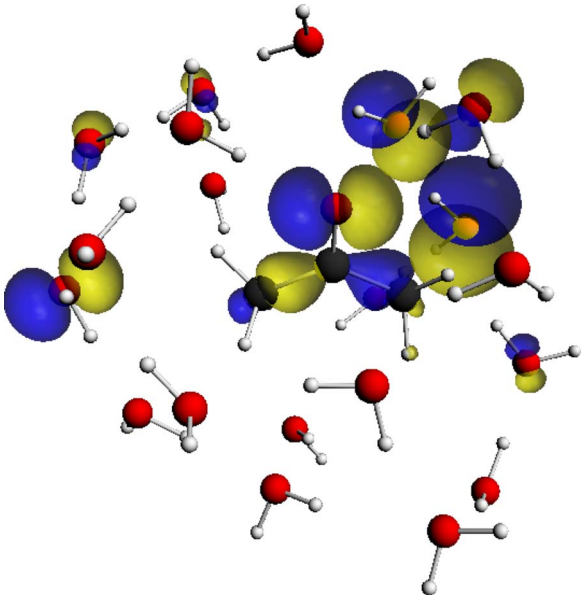

FIG. 9. Structure of the acetone-water cluster and isosurface plot of one of the orbitals with a partial $O_{acetone}$ lone pair character ($111a$).

ture of a snapshot from a Car-Parrinello molecular dymanics (CPMD) simulation, which was already studied in Ref. 17. As was demonstrated in that work, there are—in a conventional TDDFT calculation (ALDA kernel)—many low-lying excitations of charge-transfer type for this system, e.g., excitations from the water-oxygen lone pairs to the π^* orbital of the carbonyl group. Nineteen spuriously low excitations could be found for this system below the first valence transition of acetone, the $n \rightarrow \pi^*$ excitation.

Table II contains the excitation energies for all excitations up to the one which is identified as the $n \rightarrow \pi^*$ valence excitation of acetone according to the transition density overlap criterion defined in Ref. 17. A characterization of the molecular orbitals involved is given in Table III. In case of the conventional TDDFT calculation, there are many low-lying excitations of charge-transfer type. In particular, transitions from O_{water} lone pairs to the acetone π^* (e.g., 4, 5, or 10) and transitions from O_{water} lone pairs to a Rydberg-type orbital involving hydrogen atoms on a different water fragment (e.g., 1, 2, or 3) can be recognized. All of these transitions are shifted upwards when applying the asymptotic correction. The only exception is excitation 16, a transition from an O_{water} lone pair to a H_{water} Rydberg-type orbital on a neighboring water molecule. Since this Rydberg-type orbital is quite diffuse, the orbital density overlap is still five times larger than the parameter S_c, and no significant correction is applied to this transition.

The identification of acetone valence transitions is more difficult, since there is no molecular orbital of the cluster that can clearly be identified with the $O_{acetone}$ lone pairs. Instead,

TABLE III. Characterization of the orbitals (SAOP/TZP/DZ) of the acetone-water cluster shown in Fig. 9.

Orbitals	Description	Occupied Virtual
$107a-109a$	O_{water} lone pairs	Occupied
$110a-113a$	$O_{acetone}$ lone pairs+O_{water} lone pairs	Occupied
$114a-116a$	O_{water} lone pairs	Occupied
$117a$	H_{water} Rydberg	Virtual
$118a$	acetone π^*	Virtual
$119a, 120a$	H_{water} Rydberg	Virtual

TABLE II. Excitation energies (SAOP/TZP/DZ; in units of eV) of the lowest transitions of the acetone-water cluster shown in Fig. 9 from a conventional TDDFT calculation ("conv.") and calculations with the asymptotic correction. In the latter case, we either used the default switching parameter $S_c=0.0001$ or a larger value of $S_c=0.0005$. Also given are the oscillator strengths (in a.u.) from the conventional calculation and the dominant orbital contributions; the orbitals are characterized in Table III.

n	Orbitals	f	conv.	$S_c=0.0001$	$S_c=0.0005$
1	$116a \rightarrow 117a$	0.000 03	3.4344		
2	$115a \rightarrow 117a$	0.000 02	3.5271		
3	$114a \rightarrow 117a$	0.000 12	3.8155		
4	$116a \rightarrow 118a$	0.000 34	3.8657		
5	$115a \rightarrow 118a$	0.000 94	3.9600		
6	$113a \rightarrow 117a$	0.001 16	3.9747		
7	$112a \rightarrow 117a$	0.000 25	3.9873		
8	$111a \rightarrow 117a$	0.000 59	4.1768		
9	$110a \rightarrow 117a$	0.000 20	4.2072		
10	$114a \rightarrow 118a$	0.000 40	4.2471		
11	$109a \rightarrow 117a$	0.000 11	4.3690		
12	$112a \rightarrow 118a$	0.001 05	4.4218	4.4218	4.7863
13	$116a \rightarrow 119a$	0.000 12	4.4366		
14	$115a \rightarrow 119a$	0.001 25	4.5343		
15	$113a \rightarrow 118a$	0.010 66	4.5417	4.5414	4.5167
16	$108a \rightarrow 117a$	0.006 98	4.5980	4.5981	
17	$107a \rightarrow 117a$	0.002 03	4.6313		
18	$110a \rightarrow 118a$	0.000 34	4.6325	4.6329	
19	$116a \rightarrow 120a$	0.000 16	4.6668		
20	$111a \rightarrow 118a$	0.004 22	4.7112	4.7106	4.6875

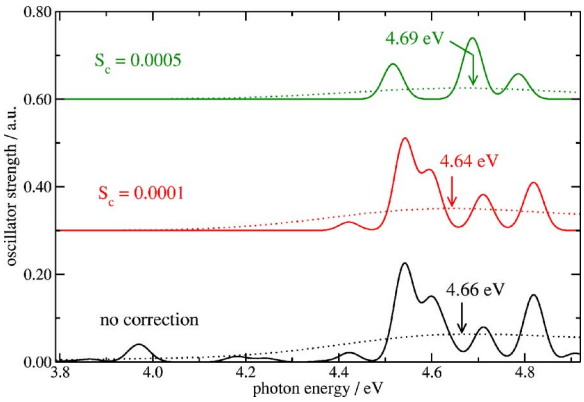

FIG. 10. Spectra (SAOP/TZP/DZ) of the acetone·20 H_2O cluster shown in Fig. 9 from a conventional TDDFT calculation ("no correction") as well as from two calculations using the asymptotic correction to the coupling matrix with different values of the switching parameter S_c. The spectra are modeled by applying a Gaussian broadening of 0.50 eV (dotted lines) and 0.05 eV (solid lines). For the spectra with a half width of 0.50 eV, also the positions of the maxima are indicated.

these lone pairs mix with O_{water} lone pairs to form the orbitals $110a-113a$, where orbitals $111a$ and $113a$ have the largest contribution from the $O_{acetone}$ lone pairs. One of these orbitals ($111a$), which are delocalized into the solvent region, is shown in Fig. 9. Transitions from all these four orbitals with a partial $O_{acetone}$ lone pair character to the acetone π^* ($118a$) orbital are basically unaffected by the asymptotic correction with the default switching parameter. Using the transition density overlap criterion defined in Ref. 17, we find that the excitation at 4.71 eV has the largest overlap with the $n\rightarrow\pi^*$ excitation of the isolated acetone molecule. This is in quite close agreement with a frozen-density embedding calculation on this cluster, which resulted in a $n\rightarrow\pi^*$ excitation energy for acetone of 4.78 eV.[17] By construction, no long-range charge-transfer problem can occur in these frozen-density embedding calculations.

In order to study the influence of the switching parameter, which was determined for the He···Be system, on such excitations with a mixed character, we increased S_c to 0.0005 in a second calculation. The effect is that the CT excitation to the Rydberg-type orbital is shifted out of this energy range, and also transitions 12 and 18 are shifted considerably, since the occupied orbitals for these transitions have only a small orbital density overlap with the acetone π^* orbital. However, the overlap is larger for orbital $112a$ and the corresponding correction is smaller, so that transition 12 is still close in energy to the other two orbital transitions with a partial $n\rightarrow\pi^*$ valence excitation character. No significant corrections result for the orbital transitions $113a\rightarrow118a$ and $111a\rightarrow118a$, but their excitation energies still change a bit because of couplings with each other and with the $112a\rightarrow118a$ transition.

Simulated spectra resulting from the uncorrected calculation as well as from the two calculations with different switching parameters for the asymptotic correction are shown in Fig. 10. The spectra are represented with a Gaussian broadening of half widths of 0.50 eV (dotted curves) and 0.05 eV (solid curves). The former broadening is often applied to achieve a better comparability with structureless experimental spectra, especially in solution, while the latter allows to distinguish the different contributing excitations. Two important conclusions can be drawn from this picture. First, the default switching parameter does not very much affect the oscillator strengths of the transitions with the highest intensities in this energy range (all transitions have rather low oscillator strengths on an absolute scale), although most of the low-lying transitions are shifted away. If the switching parameter is increased, also excitations with relatively high intensities are shifted away, and the intensity pattern of the individual transitions changes significantly. Also the total intensity decreases. However, in all three cases the maximum of the "broad" curve, i.e., the one with a half width of 0.50 eV applied to each transition, is relatively stable at 4.67 ± 0.03 eV. The default parameter of $S_c=0.0001$ a.u. is, thus, a safe choice which will not lead to the correction of excitations that cannot unambiguously be identified as charge-transfer transitions.

VI. CONCLUSIONS

The simple asymptotic correction to the exchange-correlation kernel (f_{xc}) of TDDFT suggested in Ref. 9 was shown to lead to a qualitatively correct Coulombic behavior of CT excitation energies for long distances. For particular CT transitions, it is possible to find optimal values for Δ_a which describe the correction to be applied to the conventional ALDA kernel in the asymptotic limit. With such optimized Δ_a, it is possible to obtain the excitation energies of CT states with good accuracy, provided that the orbital energy differences from the ground-state DFT calculation are reliable. For systems with many CT excitations, the simple choice to approximate Δ_a by the negative orbital energy of the accepting orbital still leads to the correct Coulombic behavior of all low-lying CT excitations with an increasing distance between the subsystems. A problem can, however, arise in cases with a strong delocalization, where the orbital density overlap criterion used here is not applicable, as has been shown for the ethylene-tetrafluoroethylene system at intermediate distances.

The present correction scheme is computationally simple and can be applied to rather large systems. In particular, calculations for molecules in solution will benefit from this correction, which automatically distinguishes between CT and non-CT transitions on the basis of the orbital density overlap. The example for acetone surrounded by water demonstrates that the resulting spectrum is only moderately affected by applying the asymptotic correction, while it is cleaned from many unphysically low excitations. The default choice of the parameter S_c and the switching function used in this study correspond to a "safe" type of correction, since excitations are only corrected if they are definitely of CT type. In doubtful cases, e.g., involving transitions to delocalized virtual orbitals, the conventional ALDA-TDDFT results are obtained, so that the correction scheme never makes the results accidentally worse than before.

The possibility of identifying CT excitations according to the orbital density overlap of the occupied and virtual orbitals involved also opens up the way to an even simpler

computational scheme, in which the corresponding orbital pairs are removed from the basis in which the $\mathbf{\Omega}$ matrix is diagonalized. Since all couplings with other orbital transitions disappear due to the zero differential overlap, their excitation energies can be calculated directly from the orbital energy differences and the simple diagonal correction applied here.

ACKNOWLEDGMENT

One of the authors (J.N.) acknowledges funding by a Forschungsstipendium of the Deutsche Forschungsgemeinschaft (DFG).

[1] A. Rosa, G. Ricciardi, O. V. Gritsenko, and E. J. Baerends, *Structure and Bonding* (Springer, Berlin, 2004), Vol. 112, pp. 49–116.
[2] K. Burke, J. Werschnik, and E. K. U. Gross, J. Chem. Phys. **123**, 062206 (2005).
[3] A. Dreuw and M. Head-Gordon, Chem. Rev. (Washington, D.C.) **105**, 4009 (2005).
[4] M. E. Casida, in *Recent Advances in Density Functional Methods Part I*, edited by D. P. Chong (World Scientific, Singapore, 1995), pp. 155–192.
[5] M. E. Casida, F. Gutierrez, J. Guan, F.-X. Gadea, D. Salahub, and J.-P. Daudey, J. Chem. Phys. **113**, 7062 (2000).
[6] D. Tozer, J. Chem. Phys. **119**, 12697 (2003).
[7] A. Dreuw, J. L. Weisman, and M. Head-Gordon, J. Chem. Phys. **119**, 2943 (2003).
[8] Y. Tawada, T. Tsuneda, S. Yanagisawa, T. Yanai, and K. Hirao, J. Chem. Phys. **120**, 8425 (2004).
[9] O. Gritsenko and E. J. Baerends, J. Chem. Phys. **121**, 655 (2004).
[10] N. T. Maitra, J. Chem. Phys. **122**, 234104 (2005).
[11] L. Bernasconi, M. Sprik, and J. Hutter, J. Chem. Phys. **119**, 12417 (2003).
[12] L. Bernasconi, M. Sprik, and J. Hutter, Chem. Phys. Lett. **394**, 141 (2004).
[13] A. Dreuw, G. R. Fleming, and M. Head-Gordon, J. Phys. Chem. B **107**, 6500 (2003).
[14] A. Dreuw, G. R. Fleming, and M. Head-Gordon, Phys. Chem. Chem. Phys. **5**, 3247 (2003).
[15] A. Dreuw and M. Head-Gordon, J. Am. Chem. Soc. **126**, 4007 (2004).
[16] S. J. A. van Gisbergen, J. G. Snijders, and E. J. Baerends, Comput. Phys. Commun. **118**, 119 (1999).
[17] J. Neugebauer, M. J. Louwerse, E. J. Baerends, and T. A. Wesolowski, J. Chem. Phys. **122**, 094115 (2005).
[18] T. Yanai, D. P. Tew, and N. C. Handy, Chem. Phys. Lett. **393**, 51 (2004).
[19] J. Neugebauer, C. R. Jacob, T. A. Wesolowski, and E. J. Baerends, J. Phys. Chem. A **109**, 7805 (2005).
[20] C.-O. Almbladh and U. von Barth, Phys. Rev. B **31**, 3231 (1985).
[21] D. P. Chong, O. V. Gritsenko, and E. J. Baerends, J. Chem. Phys. **116**, 1760 (2002).
[22] K. J. H. Giesbertz, J. Neugebauer, O. Gritsenko, and E. J. Baerends (unpublished).
[23] E. R. Davidson, J. Comput. Phys. **17**, 87 (1975).
[24] C. W. Murray, S. C. Racine, and E. R. Davidson, J. Comput. Phys. **103**, 382 (1992).
[25] C. Fonseca Guerra, J. G. Snijders, G. te Velde, and E. J. Baerends, Theor. Chem. Acc. **99**, 391 (1998).
[26] ADF, Amsterdam density-functional program, Department of Theoretical Chemistry, Vrije Universiteit, Amsterdam (URL: http://www.scm.com).
[27] G. te Velde, F. M. Bickelhaupt, E. J. Baerends, C. Fonseca Guerra, S. J. A. van Gisbergen, J. G. Snijders, and T. Ziegler, J. Comput. Chem. **22**, 931 (2001).
[28] P. R. T. Schipper, O. V. Gritsenko, S. J. A. van Gisbergen, and E. J. Baerends, J. Chem. Phys. **112**, 1344 (2000).
[29] O. V. Gritsenko, P. R. T. Schipper, and E. J. Baerends, Chem. Phys. Lett. **302**, 199 (1999).
[30] O. V. Gritsenko, P. R. T. Schipper, and E. J. Baerends, Int. J. Quantum Chem. **76**, 407 (2000).
[31] A. D. Becke, Phys. Rev. A **38**, 3098 (1988).
[32] J. P. Perdew, in *Electronic Structure of Solids*, edited by P. Ziesche and H. Eschrig (Akademie Verlag, Berlin, 1991), p. 11.
[33] C.-G. Zhan, J. A. Nichols, and D. A. Dixon, J. Phys. Chem. A **107**, 4184 (2003).
[34] See EPAPS Document No. E-JCPSA6-124-302618 for an additional figure. This document can be reached via a direct link in the online article's HTML reference section or via the EPAPS homepage (http://www.aip.org/pubservs/epaps.html).
[35] O. Christiansen, H. Koch, and P. Jørgensen, Chem. Phys. Lett. **243**, 409 (1995).
[36] O. Christiansen, H. Koch, A. Halkier, P. Jørgensen, T. Helgaker, and A. Sanchez de Meras, J. Chem. Phys. **105**, 6921 (1996).
[37] A. Schäfer, H. Horn, and R. Ahlrichs, J. Chem. Phys. **97**, 2571 (1992).
[38] A. Schäfer, C. Huber, and R. Ahlrichs, J. Chem. Phys. **100**, 5829 (1994).
[39] T. Helgaker, H. J. A. Jensen, P. Jörgensen *et al.*, DALTON, Release 2.0, a molecular electronic structure program, 2005; see http://www.kjemi.uio.no/software/dalton/dalton.html
[40] W. Hieringer and A. Görling, Chem. Phys. Lett. **419**, 557 (2006).